

University of Minnesota Morris Digital Well

University of Minnesota Morris Digital Well

---

Senior Seminars and Capstones

Student Scholarship

---

9-2-2024

## Luminescent Coupling in Perovskite Tandem Solar Cells: The Advantages of Perovskite and Luminescent Coupling in Photovoltaics

Briana Dokken

Follow this and additional works at: <https://digitalcommons.morris.umn.edu/capstone>



Part of the [Engineering Physics Commons](#), and the [Materials Science and Engineering Commons](#)

---

# **Luminescent Coupling in Perovskite Tandem Solar Cells; the advantages of perovskite and luminescent coupling in photovoltaics**

## **Introduction**

Multijunction or tandem solar cells are photovoltaic cells made of multiple semiconductor light absorbing layers. The advantage of having multiple absorber layers in a solar cell is the potential for the cell to absorb a larger range of the solar spectrum. If the absorber layers are correctly matched so that one layer absorbs low energy light while the other layer(s) absorbs high energy light, the tandem cell can absorb more light than single absorber cells. This can allow for tandem cells to have higher short-circuit currents ( $J_{sc}$ ), open-circuit voltages ( $V_{oc}$ ), and power conversion efficiencies (PCEs) while using similar amounts of materials and space as single junction cells. The first tandem solar cell was created in 1979, and it consisted of a layer of *Aluminum gallium arsenide* and a layer of *gallium arsenide* connected through a tunnel junction. As of 2020, the highest power conversion efficiencies for tandem solar cells were over 40% for tandem solar cells with six absorber layers.

While about 95% of commercial solar cells are single-junction silicon cells, many other materials are being researched for use in both single-junction and tandem cells. One material being actively researched for photovoltaic application is perovskite. Perovskites are materials with the composition  $ABX_3$  where A is a monovalent cation, B is a divalent cation, and X is a monovalent anion. Perovskite tandem solar cells have been gaining research interest due to certain perovskites' tunable bandgap, long-range charge transport, and high absorption [1]. The bandgaps of inorganic-organic perovskites can be tuned from 1.2-2.2 eV by adjusting the composition of their A, B, and X ions. Additionally, perovskites are ferroelectric, so they can hold a polarization without an applied external electric field [6]. If light can induce a voltage in a perovskite through the photovoltaic effect, perovskite could hold that voltage which is helpful for use in solar cells. Perovskites can be paired with Silicon, other perovskites, or other absorber layers for use in tandem cells. Silicon is a potentially good material to pair with perovskites in tandem cells because the silicon refining process has been optimized over the past decades. The first Silicon-perovskite tandem solar cells created in 2014 had efficiencies of 14%, and as of 2023, researchers have created perovskite-silicon tandem solar cells with efficiencies of 33.7% [13]. While this paper will only focus on perovskites in tandem solar cells, perovskites can also be used as the absorber layers in single junction solar cells, and as of 2023, single-layer perovskite solar cells have reached PCEs of 25.7% [2].

One effect that has been studied in perovskite tandem solar cells, and tandem solar cells in general, is luminescent coupling. When electrons recombine or move to lower electronic energy level states in the top layer of a tandem solar cell, they can emit photons that can be absorbed by the bottom junction of the cell, which is a process called luminescent coupling. Luminescent coupling increases the amount of light incident on the bottom junction of tandem solar cells, so it can change the output of the cells.

Perovskites and luminescent coupling are areas of active research in understanding and improving the performance of tandem solar cells. Using perovskites and increasing the luminescent coupling between tandem cell junctions has the potential to increase the voltage, current, and efficiency of solar cells. This paper will first discuss how single junction and

tandem solar cells operate, then look at the advantages of using perovskite materials in tandem solar cells and will finally look at three studies on the impacts of luminescent coupling in tandem solar cells.

### Photovoltaic Cell Operation

To understand why the use of perovskites and the tandem cell structure can increase the efficiency and power output of solar cells, it's important to understand how a single-layer solar cell functions. Light incident on a solar cell generates both a voltage and a current, which allows the cell to output power. A single layer solar cell consists of a single PN junction made of an n-doped semiconductor layer and a p-doped semiconductor layer stacked together. Semiconductors have a conduction band and a valence band that are separated by a bandgap. The conduction band of a material is a set or band of electronic energy states that have energy levels that are all close together (the states have similar energies). The valence band is another set of energy states that are close together in energy level, but the states making up the valence band are at lower energies than the conduction band states. Semiconductors are materials that have an energy difference between their conduction and valence bands of about 1 eV. The difference between the energy of the conduction band and the energy of the valence band is called the band gap of the semiconductor. In a band diagram of a semiconductor, the band gap is the energy difference between the valence and conduction bands, and there are no electronic energy states in the bandgap. Fig. 2. shows an energy band diagram of a semiconductor, with the highest valence band energy level labeled  $E_v$ , the lowest conduction band energy level labeled  $E_c$ , and the bandgap energy labeled  $E_g$ .

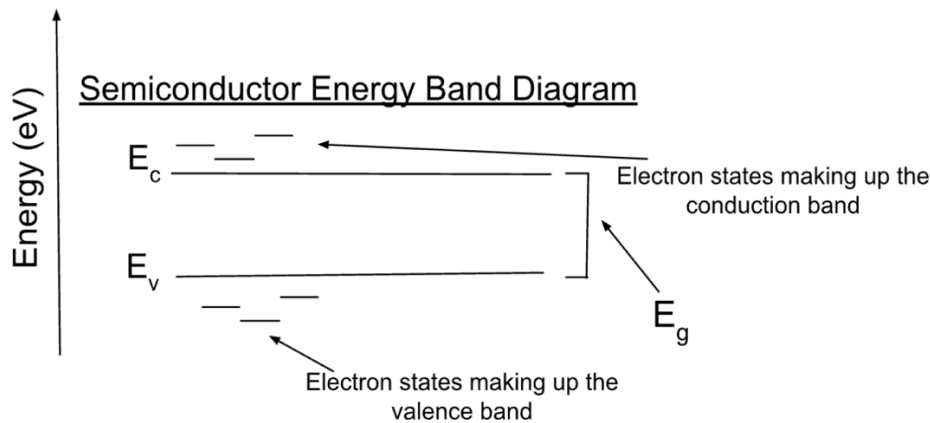


Fig. 2. A band diagram of a semiconductor with the highest valence band energy level  $E_v$ , lowest conduction band energy level  $E_c$ , and band gap energy  $E_g$ .

At 0K, the conduction band states of a semiconductor are unoccupied, and the valence band states are occupied by electrons. As the temperature of the semiconductor increases, which states ( $\epsilon$ ) are occupied follows the Fermi-Dirac distribution in Eq. 1. below

$$n(\epsilon) = \frac{1}{1 + e^{\frac{-(\epsilon - \epsilon_f)}{kT}}} \text{ Eq. 1.}$$

where  $n(\epsilon)$  is the number of electrons in the energy state with energy  $\epsilon$ ,  $\epsilon_f$  is the Fermi energy of the semiconductor (the energy difference between the highest occupied molecular orbital (HOMO) and lowest unoccupied molecular orbital (LUMO) of the semiconductor),  $k$  is Boltzmann's constant, and  $T$  is the temperature of the semiconductor. Since electrons are Fermions, the number of electrons per state  $\epsilon$  can be 0 or 1. For energy states below  $\epsilon_f$  (valence band states),  $n(\epsilon)$  equals 1 when  $T=0K$ . For energy states above the Fermi energy ( $\epsilon > \epsilon_f$ ), when  $T=0K$   $n(\epsilon)=0$ , which means there are no electrons in any of the conduction band states. As  $T$  increases above  $0K$ , the distribution of electrons shifts, and some of the electrons in the upper valence band states are thermally excited up into the lower conduction band states. The number of electrons  $n(\epsilon)$  in each state  $\epsilon$  at  $T=0K$  and at a temperature  $T$  greater than  $0K$  are shown in Fig. 3 below.

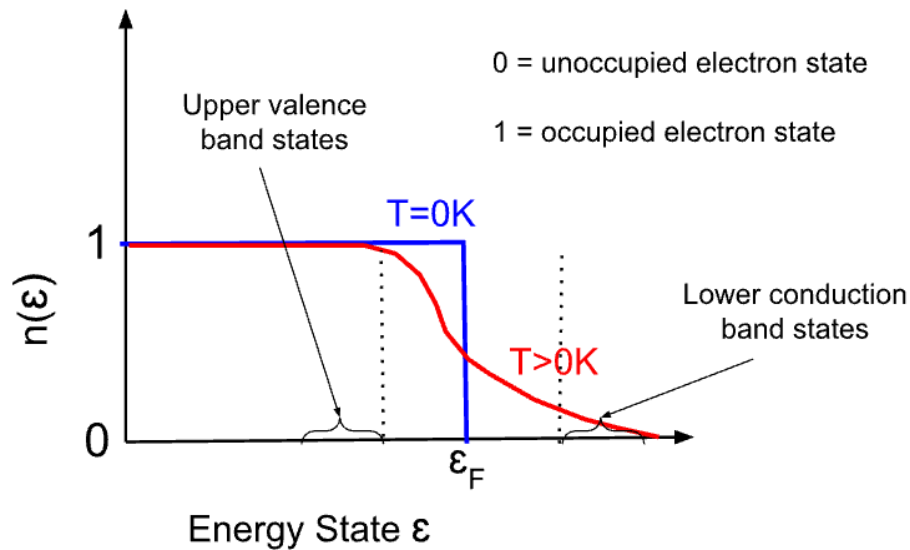


Fig. 3  $n(\epsilon)$  vs  $\epsilon$  for a temperature  $T=0K$  and  $T>0K$

The Fermi-Dirac distribution shows that when an external source of energy is provided to a semiconductor, the energy can be absorbed by electrons in the valence band states, and these electrons are then excited up into previously unoccupied conduction band states. This leaves the valence band state unoccupied. In solar cells, semiconductors are used because exciting electrons from lower to higher energy states creates a voltage and current across the cell.

Solar cells consist of a PN junction that is made of a p-doped and an n-doped semiconductor layers that are physically connected. P-doped semiconductors are semiconductors that have atoms (impurities) added in that have open electronic energy states (defect states) in the bandgap that are only slightly higher in energy than the valence band energy level. This allows electrons from the higher valence band states to be easily excited up to these defect states and leave behind "holes" (spots where the electrons were) in the valence band states. N-doped semiconductor materials have atoms (impurities) added in that have extra filled electronic energy states (defect states) with energies slightly lower than the lowest

unoccupied conduction band states. Electrons in these defect states can be easily excited into unoccupied, lower conduction band states. A band diagram of a p-doped and an n-doped semiconductor are shown below in Fig. 4.

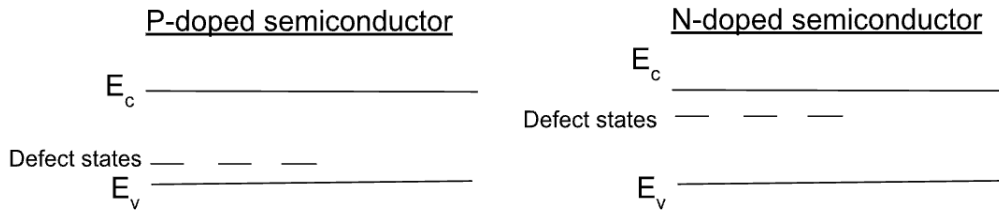


Fig. 4. Locations of defect states in a p-doped semiconductor (these defect states are unoccupied electron energy levels) and locations of defect states in an n-doped semiconductor (these defect states are occupied electron energy levels). The vertical axis represents the energy of these states (higher vertically on the band diagram shows a greater energy level).

When the p-doped and n-doped semiconductors are physically brought together, a PN junction is formed. Right after the layers are brought together, electrons from the n-doped material's conduction band diffuse into the p-doped material's conduction band, since there is initially a higher concentration of electrons in the n-type layer's conduction band than in the p-type layer's conduction band. Holes, "open spots" where electrons used to be, diffuse from the p-type layer's valence band into the n-type layer's valence band, since the p-type layer's valence band initially has a higher concentration of holes than the n-type layer's valence band. Both the p-doped and n-doped layers are individually electrically neutral, but the gradient of carrier (hole and electron) concentrations cause a diffusion of electrons to the p-doped side of the junction and a diffusion of holes to the n-doped side of the junction. This is shown below in Fig. 5.

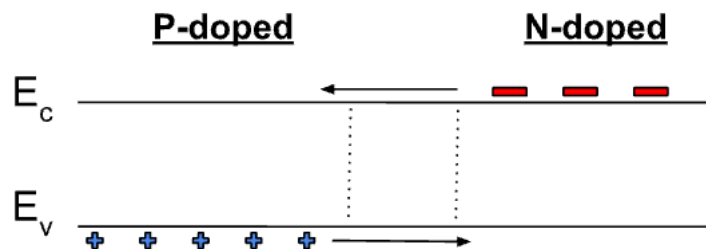


Fig. 5. An energy band diagram of a PN junction right after the P and N-doped layers are connected. Electrons are represented as the red negative signs diffusing from the n-doped conduction band to the p-doped conduction band, and holes are represented as blue plus signs diffusing from the p-doped valence band to the n-doped valence band.

The build-up of holes on the edge of the n-doped layer (next to the junction) and the build-up of electrons on the edge of the p-doped layer (next to the junction) leads to a potential difference between the n-doped and p-doped layers. The build-up of holes and electrons on opposite sides of the PN junction is shown in Fig. 6 below.

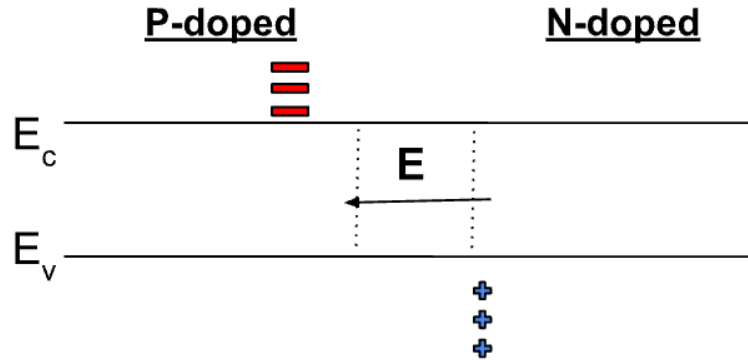


Fig. 6. An energy band diagram of a PN junction after electrons have diffused from the n-doped conduction band to the p-doped conduction band, and holes have diffused from the p-doped valence band to the n-doped valence band. The build-up of opposite charges on either edge of the junction creates the internal electric field  $E$ . The edge of each layer is marked with a dotted line, and the area between the two lines is called the depletion region. Charges in the depletion region are swept to either side of the junction by  $E$  and do not stay in that region.

Holes will continue to diffuse to the n-type side and electrons will continue to diffuse to the p-type side until the internal electric field (labeled  $E$  in Fig. 6) generated from these built-up charges gets strong enough to prevent further diffusion. The buildup of positive charges at the edge of the n-doped side of the junction causes the n-doped layer to have a higher potential than the p-doped layer, and this can be shown as “band bending” in the energy band diagram in Fig. 7.

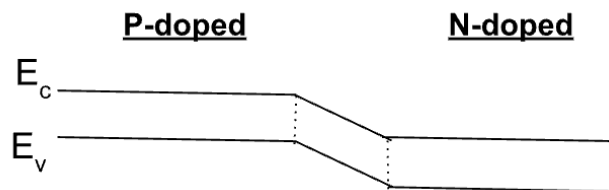


Fig. 7. The energy bands of the p and n-doped semiconductors after the internal electric field and potential difference are established (this happens once the two layers have been in contact long enough for net diffusion to start and end). In an energy band diagram, the side where the electrons are at a higher potential is shown as vertically higher. Since the n-doped side of the junction is at a higher potential overall, the n-doped side has a lower potential for negatively charged electrons. The junction shown has “bent” energy bands.

Another way to visualize the band bending at a PN junction is through differences in Fermi energy levels. The Fermi energy of a semiconductor is the difference in energy between the highest occupied molecular orbital (HOMO) and lowest unoccupied molecular orbital (LUMO). In the p-doped material, the Fermi energy level is right above the semiconductor's valence band, and in the n-doped material, the Fermi energy level is right below the conduction band. A higher potential leads to a higher Fermi level, so the n-doped layer has a higher Fermi energy level than the p-doped layer. When the p and n-doped semiconductors are brought together, the valence band and conduction bands of each "bend", to create one Fermi level for the PN junction. The n-doped side is still at the higher potential for positive charges, so negatively charged electrons have a lower potential at the n-doped side of the junction. This is represented as the n-doped side being lower than the p-doped side in the PN junction band diagram.

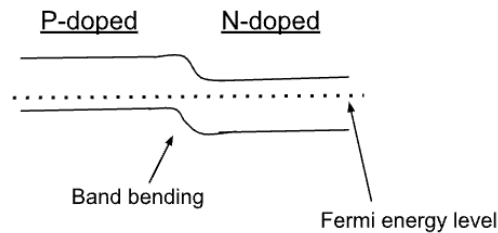


Fig. 4. Band diagram of a PN junction, with the Fermi energy level of the material shown as the dotted line.

For current to continuously flow from a PN junction, an external source is needed to regenerate extra holes in the p-doped valence band and extra electrons in the n-doped conduction band. In PN junction solar cells, photons from light can regenerate these excess electrons and holes. When photons from light are absorbed by electrons in the defect energy states next to the n-doped region's conduction band, the electrons are excited up into the n-doped region's conduction band, and once again the n-doped conduction band has more electrons than the p-doped conduction band. When photons are absorbed by electrons in the valence band of the p-doped material, the electrons can be excited up into the extra defect energy levels in the p-doped material, leading to the valence band of the p-doped material having more holes than the valence band of the n-doped material. This once again makes the p-doped material's potential lower than the n-doped material's potential, and electrons can flow from the conduction band of the n-doped material to the p-doped material and through an external circuit. Light incident on the solar cell can regenerate photo-excited carriers, regenerating a potential difference across the PN junction, which leads to a current flowing from the solar cell that is able to power an external load.

The current for the solar cell is provided when electrons in the PN junction's valence band absorb photons with energy equal to or greater than the band gap of the junction and get excited into states in the junction's conduction band. These electrons and the holes they leave behind are considered free charge carriers that can contribute to current [12].

Photons absorbed by electrons can regenerate a voltage in the photovoltaic cell by exciting electrons up from the n-doped defect states to the n-doped conduction band and up from the p-doped valence band to the p-doped defect states. When electrons go from a higher energy state back down to lower energy states, the electrons “recombine” with the holes they left behind in the lower energy state. When a previously excited electron goes through recombination, it goes back down to the lower energy state it was previously in. There are a variety of mechanisms of recombination in semiconductors, and one of these mechanisms is radiative recombination. During radiative recombination, the energy lost by the electron going from a higher energy state to a lower energy state is emitted as a luminescent photon. This effect is particularly important in tandem, or multi-layer, solar cells.

### **Tandem Solar Cells**

Instead of having a single PN junction, tandem solar cells contain multiple PN junctions that can each absorb different energies of light. The PN junctions that make up a tandem cell are vertically stacked on top of each other. In two junction tandem solar cells, the top PN junction is made of a material with a larger bandgap and the bottom PN junction is made of a material with a smaller bandgap. Since the top semiconductor layer has a large bandgap, it can only absorb high energy photons. Low energy photons pass through the top sub cell and are absorbed by the bottom sub cell with the smaller bandgap. This allows tandem cells to absorb a wider range of the solar spectrum, giving them the potential to absorb more light and have a higher power output than single-layer solar cells.

The sub cells that compose a tandem solar cell can be connected monolithically or mechanically. In monolithic tandem solar cells, multiple sub cells are fabricated on top of one another and are connected through tunnel junctions. On the other hand, in mechanical tandem solar cells, sub cells are fabricated separately and then combined. Each sub cell in a mechanical tandem cell has its own set of contacts, so current is collected separately from each layer. In monolithic cells, each sub cell is connected in series like resistors, so the current coming out of the entire cell is equal to the lowest current coming from one of the sub cells. To maximize the current output by a monolithic cell, all the sub cells should have the same current, which is a condition called current matching. Since the sub cells are not connected in series in mechanically stacked cells, current matching is not relevant for mechanical cells. Current matching is a major factor that impacts the optimal thickness and bandgap of the sub cells in monolithic tandems. Some advantages of monolithic over mechanical cells are the reduced cost of production from only having to create two contacts for the cell, the reduced parasitic absorption in the cell at contacts (since there are less contacts in monolithic cells), and the ability of more easily integrating monolithic cells into photovoltaic systems since they contain 2 terminals. The tandem cells focused on in the rest of this paper are monolithic cells that require current matching.

## **Luminescent Coupling in Tandem Solar Cells**

When radiative recombination happens in the top junction of a tandem solar cell, the photons emitted can be absorbed by the bottom junction, as long as they have an energy equal to or greater than the bandgap of the bottom junction. The absorption of photons by the bottom junction that were produced by radiative recombination in the top junction is called luminescent coupling. Luminescent coupling increases the current coming out of the bottom junction, so it has an impact on the maximum current, voltage, and efficiency of monolithic tandem solar cells.

## **Perovskites in Photovoltaics**

The majority of solar panels are made of silicon, and about 95% of modules sold are silicon solar panels [14]. Silicon has an optimal bandgap of 1.1 eV, which allows it to absorb photons with wavelengths of 1130 nm and above. It is also one of the most abundant elements, it is not toxic, and crystalline silicon is stable. Silicon solar panels typically have lifetimes of about 25 years [14], which is one of the longest for commercial solar panels.

While these factors make silicon the most commonly used material for absorber layers in commercial solar cells, a wide variety of other materials are being researched for other advantages as well. One material that is currently researched for use in solar cells is perovskite. Perovskites are a category of materials that have the general formula  $ABX_3$ , where X is either oxygen or a halogen (F, Cl, Br, etc.), A is a larger cation, and B is a smaller cation. The A cation is located in a cubo-octahedral site and the B cation is located in an octahedral site, creating the structure shown in Fig. 7. below.

This image is under copyright. It can be viewed online in the publication “Perovskite solar cells: An emerging photovoltaic technology” Nam-Gyu Park. Figure 2 (a).

Fig. 7. Perovskite unit cell structure

Perovskite materials are of interest, specifically for thin-film photovoltaics, because of the materials' ability to perform well even with defects. Silicon requires a high grade of purity to be used in electronics, while perovskite materials can contain more defects and still function in photovoltaic cells [8]. Additionally, perovskites can have high absorption coefficients, which means that light incident on a perovskite layer is absorbed near the top of the layer. This allows perovskite layers to absorb a significant amount of the solar spectrum even when they are thin, making them a good candidate for thin-film solar cells. Additionally, perovskite layers can have narrow and tunable bandgaps, allowing them to absorb lower energy photons that would pass through materials with larger bandgaps. By changing the composition of the ions in the perovskite or using multiple halogens blended for the X ion, researchers can adjust the bandgap of perovskites, which is useful for perovskites in tandem solar cells. Perovskites also have long diffusion lengths (the length an electron can travel before relaxing down to a lower energy state).

Finally, perovskites have high dielectric constants, which leads to low exciton binding energies [1] and a higher potential across the material. Currently, perovskite cells are not commercially available because 3D perovskites are not stable [2], but they are an active area in photovoltaic research.

Perovskites with an oxygen X anion are particularly advantageous for use in solar cells because of the material's ferroelectricity. Ferroelectric materials are made of crystals that can hold a dipole moment in the absence of an external electric field. Hysteresis curves have been measured in perovskite, which shows that perovskites are ferroelectric. Hysteresis curves are the loops on a graph of a material's polarization (charge per unit area) versus the electric field applied to the material. Fig. 8 below shows the measured hysteresis curves. While ferroelectric materials can be useful for solar cells, hysteresis curves present a challenge because cells with these curves have different voltages depending on which direction they are scanned (which direction the external electric field is originally applied). While eliminating these hysteresis curves are a current challenge of perovskite solar cells, the material's ferroelectricity can still work as an advantage in photovoltaics.

This image is under copyright. It can be viewed online in the publication "Polarization twist in perovskite ferroelectrics" by Yuuki Kitanaka et al. Figure 1.

Fig. 8. Hysteresis curves in perovskite (polarization vs electric field) [15].

Ferroelectric materials are useful for photovoltaics because they can enhance the charge separation of electron-holes pairs that carry current from the solar cell. The internal electric field held by ferroelectric materials can be 1 to 2 orders of magnitude greater than the electric field strength at a non-ferroelectric PN junction. The internal electric field is also found throughout the ferroelectric material, further allowing ferroelectrics to increase charge carrier separation in solar cells [1]. "Nalwa et al. reported that doping with ferroelectrics leads to localized enhancements of electric field in photovoltaic active-layer with a resulting internal quantum efficiencies [ratio of total electron-hole pairs generated to photons absorbed] of ca. 100%, and the PCE of the solar cell is consequently increased by nearly 50%, indicating a much more efficient dissociation of singlet-excitons and charge-transfer-excitons as the result of the enhanced electric field" [1]. If a perovskite's polarized form is favorable, it can be ferroelectric and useful for separating charge carriers as an absorber layer in photovoltaic solar cells.

Since a number of perovskites are ferroelectric, there is a physical property of perovskite that makes its polarized form favorable. To see why the polarized structure of a perovskite with oxygen is physically favored, we can compare the dielectric constant of a perovskite material to a known equation for the dielectric constant of any material that is ferroelectric because of a permanent dipole moment. This will determine if perovskite's ferroelectricity comes from a permanent dipole, or if there is another physical cause of perovskite's ferroelectricity.

When an external electric field is applied to a material, the atoms in the material can become polarized, and the polarization points in the same direction as the applied electric field. We will start by looking at the polarization of an individual atom, and this can then be applied to

molecules and materials. The induced polarization  $\mathbf{P}$  (dipole moment per unit volume) of an atom with an atomic polarizability  $\alpha$  by an external electric field  $\mathbf{E}$  is given by [9]

$$\mathbf{P} = \alpha\mathbf{E} \text{ Eq. 1.}$$

When an atom becomes polarized, the external applied electric field  $\mathbf{E}$  slightly shifts the positively charged nucleus of the atom in one direction and the negatively charged electron cloud in another. A second electric field is induced between the nucleus and electron cloud that points towards the direction that the electron cloud shifted in, opposite of the applied electric field. This induced field and the applied field contribute to the total electric field,  $\mathbf{E}_{total}$ , in the material.

Materials that have a polarization  $\mathbf{P}$  that is proportional to the total electric field  $\mathbf{E}_{total}$  (the net electric field from the applied field and the field induced by the polarization) are called linear dielectrics, and their polarization follows the equation

$$\mathbf{P} = \epsilon_0 \chi \mathbf{E}_{total} \text{ Eq. 2}$$

where  $\epsilon_0$  is the permittivity of a vacuum and is used to cancel out units, and  $\chi$  is the electric susceptibility (a constant of proportionality). Another value used in solving for the effects of polarization is the displacement  $\mathbf{D}$ , which can be defined as the average electric field inside a dish-shaped hole in the material that is perpendicular to the polarization. The displacement is proportional to the applied electric field

$$\mathbf{D} = \epsilon \mathbf{E}_{total} \text{ Eq. 3}$$

$$\text{with } \epsilon \equiv \epsilon_0 (1 + \chi) \text{ Eq. 4.}$$

where  $\epsilon$  is the permittivity of the material and  $\epsilon/\epsilon_0$  is the dielectric constant of the material. Eq. 4. is a general expression for the dielectric constant of a material with a displacement  $\mathbf{D}$ , total electric field  $\mathbf{E}_{total}$ , and electric susceptibility  $\chi$ . The known equation for the dielectric constant of any material that is ferroelectric because it contains a permanent dipole is

$$\epsilon = \frac{3Tc}{T-Tc} \text{ Eq. 5}$$

where  $T_C$  is the critical temperature, the highest temperature the material can reach before it stops being ferroelectric (at temperatures below  $T_C$  the material is ferroelectric, at temperatures above  $T_C$  the material is no longer ferroelectric).

Next, we can determine if perovskites' ferroelectricity is caused by a permanent dipole by deriving an equation for the dielectric constant of barium titanate and comparing it to Eq. 5. Barium titanate is a perovskite with a cubic unit cell that has a titanium 4+ ion at the center, barium 2+ ions at the corners, and oxygen 2- ions at the face.

To find the dielectric constant of barium titanate, we can start by calculating the perovskite's polarization  $\mathbf{P}$ . The local electric field, which is the electric field at one atom in the perovskite, is  $\mathbf{E}_{local}$ .  $\mathbf{E}_{local}$  is the net field resulting from the applied electric field  $\mathbf{E}$  and the electric field resulting from the polarization (the field that comes from the other ions acting on the atom we're looking at). The perovskite is made of different types of atoms per volume  $N_i$  which have polarizabilities  $\alpha_i$ . The total polarization of the perovskite barium titanate is equal to

$$\mathbf{P} = \sum_i E_{local} N_i \alpha_i \text{ Eq. 6}$$

where  $i$  is each of the different kinds of atoms in the perovskite.

The dielectric constant,  $\epsilon$ , of the perovskite can be found from the ratio of the field's displacement over the total electric field inside the dielectric  $\mathbf{E}_{total}$ , or

$$\epsilon = \frac{|D|}{|E_{total}|} = 1 + 4\pi \left( \frac{|P|}{|E_{total}|} \right) \text{ Eq. 7}$$

Then, if the local electric field is related to the total electric field by,

$$\mathbf{E}_{local} = \mathbf{E}_{total} + \frac{4\pi\mathbf{P}}{3} \text{ Eq. 8}$$

$\frac{\mathbf{P}}{E_{total}}$  becomes

$$\frac{\mathbf{P}}{E_{total}} = \frac{\sum_i N_i \alpha_i}{1 - \frac{4\pi}{3} \sum_i N_i \alpha_i} \text{ Eq. 9}$$

Which can be combined with Eq. 6 and rearranged for the dielectric constant  $\epsilon$  as

$$\epsilon = 1 + 4\pi \left( \frac{\mathbf{P}}{\mathbf{E}} \right) = \frac{1 + \frac{8\pi}{3} \sum_i N_i \alpha_i}{1 - \frac{4\pi}{3} \sum_i N_i \alpha_i} \text{ Eq. 10}$$

As  $\sum_i N_i \alpha_i$  approaches  $\frac{3}{4\pi}$ ,  $\epsilon$  goes to infinity, so  $\epsilon$  varies as  $\sum_i N_i \alpha_i$  becomes an amount  $s$  smaller or greater than  $3/4\pi$ . This can be represented by the equation

$$\frac{4\pi}{3} \sum_i N_i \alpha_i = 1 - s \text{ Eq. 11}$$

When  $s \ll 1$ , combining Eq.s 9 and 10 and solving for  $\epsilon$  gives

$$\epsilon \cong 3/s \text{ Eq. 12}$$

Assuming that near the critical temperature  $T_c$   $s$  varies linearly with the temperature  $T$  of the material, then it is also the case that

$$s \cong \beta(T - T_c) \text{ Eq. 13}$$

where  $\beta$  is  $1/(kT)$  ( $k$  is Boltzmann's constant) and  $T_c$  is the critical temperature. Substituting Eq. 12 into Eq. 11 gives the dielectric constant for barium titanate as

$$\epsilon \cong \frac{3/\beta}{T - T_c} \approx \frac{10^5}{T - T_c} s \cong \beta(T - T_c) \text{ Eq. 14}$$

The given equation for the dielectric constant of materials that are ferroelectric due to a permanent dipole follows

$$\epsilon = \frac{3Tc}{T-Tc} \text{ Eq. 5}$$

Since the equation for the dielectric constant of barium titanate does not match Eq. 5, the perovskite barium titanate likely does not have a permanent dipole moment that causes its ferroelectricity. When an external electric field is applied to a perovskite, including barium titanate, the differently charged cations and anions are pulled in opposite directions. When each of these ions are displaced from one another, a restoring force between the two is established. If the electric field created by this polarization increases at a faster rate than the restoring force, the ions shift asymmetrically and a dipole moment is induced. However, since Eq. 5 and Eq. 14 are not equivalent, this dipole must not be a permanent dipole causing the perovskite's ferroelectricity.

Barium titanate's induced dipole is not a permanent dipole and must not be the only factor causing the material's ferroelectricity. It can be shown that the local electric field  $E_{\text{local}}$  (the electric field on a specific atom coming from both the applied and induced fields) in perovskite increases the effects of the polarizability of the titanium ion, which is what causes the barium titanate's ferroelectricity.

To observe how the local electric fields in the barium titanate unit cell enhance the polarizability of the material and cause its ferroelectricity, we can find the percent of the perovskite's polarization that is ionic and the percent of the polarization that is electronic. Ionic polarization is polarization caused by ions that are asymmetrically displaced relative to each other after the application of an external electric field [16]. Electronic polarization is the polarization caused by negative clouds of electrons being shifted away from the positive nuclei of atoms [10]. The refractive index  $n$  for barium titanate is 2.4, which gives an electronic contribution to the polarizability from

$$\frac{n^2-1}{n^2+2} = \frac{4\pi}{3} \sum N_i \alpha_i (\text{electronic}) = 0.61 \text{ Eq. 15}$$

after plugging in given values of  $\alpha_i$  for barium, oxygen, and titanium. If the electronic contribution to the conductivity is 0.61, then the ionic contribution to the polarizability is  $1-0.61 = 0.39$ , which means that 39% of the total polarization of the barium titanate is ionic. The following derivation shows that the perovskite structure enhances the polarizability of the titanium ion that causes the 39% ionic contribution to the polarization, which is what makes the perovskite structure ferroelectric.

For barium titanate, the local electric field is equal to the sum of the local electric field at each lattice point. The local field at each lattice point is the sum of the applied field and the polarization of the ions surrounding it. The local electric field ( $E_{\text{local}}$ ) at the Ba, O' (Oxygen in line with the Ti ions), O'' (oxygen surrounding Ti ions in a square), and Ti ions are given by

$$\begin{aligned} E_{Ba} &= P_{Ba}/(N_{Ba})(\alpha_{Ba}) = \mathbf{E}_{\text{applied}} + q_{11}P_{Ba} + q_{12}P_{Ti} + q_{13}P_{O'} + q_{14}P_{O''} \\ E_{O'} &= P_{O'}/(N_{O'})(\alpha_{O'}) = \mathbf{E}_{\text{applied}} + q_{21}P_{Ba} + q_{22}P_{Ti} + q_{23}P_{O'} + q_{24}P_{O''} \\ E_{O''} &= P_{O''}/(N_{O''})(\alpha_{O''}) = \mathbf{E}_{\text{applied}} + q_{31}P_{Ba} + q_{32}P_{Ti} + q_{33}P_{O'} + q_{34}P_{O''} \end{aligned}$$

$$E_{Ti} = P_{Ti}/(N_{Ti})(\alpha_{Ti}) = \mathbf{E}_{applied} + q_{41}P_{Ba} + q_{42}P_{Ti} + q_{43}P_{O'} + q_{44}P_{O''}$$

Eq. 15

Where  $q_{xx}$  are coefficients calculated from lattice sums for dipole arrays, and have the values

$$\begin{aligned} q_{11} &= q_{22} = q_{21} = q_{12} = q_{33} = 4\pi/3 \\ q_{13} &= q_{31} = \frac{4\pi}{3} - 8.668 \\ q_{34} &= q_{43} = q_{14} = q_{41} = \frac{4\pi}{3} + 4.334 \\ q_{23} &= q_{32} = \frac{4\pi}{3} + 30.080 \\ q_{24} &= q_{42} = \frac{4\pi}{3} - 15.040 \\ q_{44} &= \frac{4\pi}{3} - 4.334 \end{aligned}$$

Eq. 16

Since  $q_{23}$  and  $q_{32}$  are much greater than  $\frac{4\pi}{3}$ , they lead to the interactions between the Ti and oxygen ions that are in line with the Ti ions (directly above and below) to be particularly strong. The strong interactions between the Ti and O' ions cause a stronger field at the central Ti ion of the perovskite.

In order for BaTiO<sub>3</sub> to be ferroelectric,  $\mathbf{E}_{applied}$  must be able to equal 0 when P does not equal 0. For this to happen, the polarizations in Eq. 15 must have nontrivial solutions when  $\mathbf{E}_{applied}$  is equal to 0, and the determinant of the  $q_{xx}$  values has to equal 0. When the determinant of these values equals 0 and we assume that the Ba, O', and O'' polarizabilities are electronic and the Ti polarizability is ionic, the value of  $\alpha_{Ti}$  that causes the determinant of the q values to equal 0 is  $0.95 \cdot 10^{-24} \text{ cm}^3$ . This leads to

$$\frac{4\pi}{3} N_{Ti} \alpha_{Ti} = 0.062 \text{ Eq. 17}$$

Which is much less than the 39% of the polarization that must be ionic. Since the ionic polarization only comes from the Ti ion, and the Ti ion's polarization (0.062) is six times less than the ionic part of the polarization (0.39), the strong electric field along the lines of the O' and Ti ions in the lattice strengthens the ionic polarization.

Another way to explain perovskites', specifically barium titanate's, ferroelectricity is that it is likely caused by a displacement of the O' and Ti ions into a meta-stable state. When an external electric field is applied to the perovskite, the positive Ti ion and the negative O ions that were originally placed along the same line are displaced slightly in opposite directions. This creates a polarization, and the Ti and O ions experience an attractive force opposing the direction of their displacement. These two forces balance out. Once the Ti and O ions settle into their displaced states, there is an energy barrier between that displaced state and the lower energy non-displaced (original) state. Since it would take energy to break the Ti and O ions from their displaced states back into their original state, for low enough temperatures (temperatures below

$T_c$ ), the ions stay in the displaced state and the perovskite remains polarized even if the external electric field is no longer applied. Since perovskites can hold a polarization without the application of an external field, they are ferroelectric and a good candidate for photovoltaic applications.

### **Studies on Luminescent Coupling in Tandem Solar Cells**

One effect in perovskite tandem solar cells that is being studied is luminescent coupling. Luminescent coupling has been observed and measured in a variety of tandem solar cells, including perovskite cells. Using perovskite materials as one or both of the layers in two junction tandem solar cells leads to devices that have the advantages of perovskite layers (band gap tunability, ferroelectricity, and high absorption coefficients), and also have the possibility of absorbing a wider range of the solar spectrum. Another advantage of creating tandem solar cells with perovskite layers is the possibility of luminescent coupling between tandem cell layers, which can boost the  $J_{sc}$  and PCE of the solar cell. This section will focus on the predicted, simulated, and measured impacts of luminescent coupling on two junction monolithic tandem solar cells, both made with perovskite and other material layers. The effects of luminescent coupling on both perovskite-silicon and GaInP-GaAs two junction tandem cells have been studied, and the results of these studies on luminescent coupling could potentially be broadly applied to tandem cells that experience luminescent coupling. Luminescent coupling also impacts the optimal thickness and bandgap of the perovskite layer in perovskite tandem solar cells, so it is important to factor in the effects of luminescent coupling when designing perovskite tandem solar panels.

### **Effects of Luminescent-Coupling on Monolithic Tandem Cells: GaInP-GaAs Cells**

The effects of luminescent coupling on GaInP/GaAs monolithic tandem solar cells can be estimated analytically and measured experimentally, and the conclusions about the impacts of these effects can be applied to luminescent coupling in tandem solar cells in general, including perovskite tandem solar cells. In “Analysis of Multijunction Solar Cell Current-Voltage Characteristics in the Presence of Luminescent Coupling”, the effects of luminescent coupling on GaInP/GaAs tandem cells were modeled analytically using the ideal diode equation with a luminescent current added, and by experimentally measuring the short circuit current ( $J_{sc}$ ), open circuit voltage ( $V_{oc}$ ), and power conversion efficiency (PCE) of GaInP-GaAs cells. The study found that luminescent coupling impacts the  $J_{sc}$ ,  $V_{oc}$ , and PCE of monolithic tandem solar cells, which is why luminescent coupling impacts the optimal design of monolithic tandem cells and is being studied in perovskite tandem solar cells.

The study first derives a set of equations needed to plot the  $J$  (current density) vs  $V$  (voltage) curves of a tandem cell that experiences luminescent coupling. The effects of luminescent coupling on the current coming from the bottom junction of the tandem cell is also modeled in “A review of modeling of luminescent coupling effect in multi-junction solar cell based on diode equation”, which follows a similar derivation [11]. From these two papers, the equation for the  $J$  vs  $V$  curves for a two-junction cell with luminescent coupling can be derived

by first finding expressions for the voltages of both sub cells, substituting a luminescent coupling current density ( $J_{LC}$ ) into that equation, and then plotting the tandem cell JV curves.

The current density (current/unit area) output by a single junction of a tandem solar cell,  $J_{out}$ , can be represented by the circuit in Fig. 8 below;

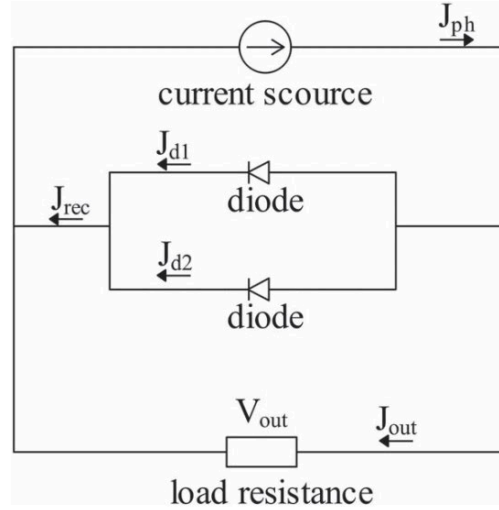


Fig. 8 The equivalent circuit of the current density output by a single junction solar cell ( $J_{out}$ ), with a total recombination current density in the cell of  $J_{rec}$ , and a photocurrent  $J_{ph}$  provided by sunlight.

The recombination current density in the single junction solar cell,  $J_{rec}$ , reduces the current density output by the cell,  $J_{out}$ , that comes from  $J_{ph}$ , so that  $J_{out} = J_{ph} - J_{rec}$ . Eq. 18 below gives the total current output by the junction (junction i)

$$J(V_i) = J_{01,i} \left[ \exp\left(\frac{eV_i}{kT}\right) - 1 \right] + J_{02,i} \left[ \exp\left(\frac{eV_i}{2kT}\right) - 1 \right] - J_{ph} \quad \text{Eq. 19}$$

The  $J_{01,i}$  and  $J_{02,i}$  terms represent the currents from diode one ( $J_{d1}$ ) and diode 2 ( $J_{d2}$ ) in Fig. 8, and are the radiative and non-radiative recombination currents in the junction.  $J_{ph}$  is set to be negative by convention, and the total current output by the cell will be 0 or negative. The equations for the recombination current densities from both of the diodes come from the ideal diode equation with an ideality factor of 1 ( $n=1$ ) for  $J_{01,i}$ , and an ideality factor of 2 ( $n=2$ ) for  $J_{02,i}$ . The equation for current density through an ideal diode is

$$J = J_0 e^{\left(\frac{qV}{nkT} - 1\right)} \quad \text{Eq. 20}$$

where  $J$  is the net current density flowing through the diode,  $J_0$  is the dark saturation current density (the current density flowing through the diode when it is in the dark),  $q$  is the absolute value of the charge of an electron,  $V$  is the applied voltage across the terminals of the diode,  $n$  is an ideality factor between 1-2 that increases as the current through the diode

decreases,  $k$  is Boltzmann's constant, and  $T$  is the temperature of the diode in kelvin [12]. The  $J_{01,i}$  term in Eq. 19 represents the radiative recombination current density in the top sub cell, and the  $J_{02}$  term represents the non-radiative recombination current density in the  $i$ th sub cell.

We can set  $J_{02}=0$ , meaning that there is no non-radiative recombination in the solar cell. This is not completely realistic but will not significantly change the result of the analysis. This changes Eq. 19, the current output by a single junction of the tandem cell, to

$$J(V_i) = J_{01,i} \left[ \exp\left(\frac{eV_i}{kT}\right) - 1 \right] - J_{Ph} \quad \text{Eq. 21}$$

We can also create a term for the luminescent coupling (LC) current density (the current density of electrons from LC being absorbed by the bottom junction), by setting the LC current density  $J_{LC}$ , as a fraction of the radiative recombination current density (the  $J_{01}$  term in Eq. 21). This gives

$$J_{LC}(J) = \eta_{i,j} J_{01,j} \left[ \exp\left(\frac{eV_j}{kT}\right) - 1 \right] \quad \text{Eq. 22}$$

as the luminescent coupling current density between the top and bottom sub cell of a tandem cell, where "j" is the index of the bottom junction ( $V_j$  is the voltage of the bottom junction) and "i" is the index of the top junction. The luminescent coupling current is a function of the current output by the entire tandem cell,  $J$ .  $\eta$  is a LC efficiency which can vary from 0 to 1 (0 being no LC between sub cells, 1 meaning that all of the radiative recombination in the top sub cell is absorbed by the bottom sub cell through LC).

If Eq. 20 is solved for  $J_{01,i}$  and then substituted into Eq. 21, we can get the following expression for the LC current between sub cells

$$J_{LC} = \eta_{i,j}(J + J_{Ph,1}) \quad \text{Eq. 23}$$

Eq. 22 is the equation that we can use to describe the LC current between the top and bottom sub cells of a two junction tandem solar cell.

Now that we have an equation for the LC current, the next step in plotting the  $J$  vs  $V$  curves of a tandem cell with LC is to find equations for the voltage of the top ( $V_i$ ) and bottom ( $V_j$ ) sub cells. To get an equation for the voltage of the top (i) sub cell, we can take the inverse of Eq. 21 to get

$$\text{Eq. 23 } V_i(J) = \frac{kT}{q} \ln\left[1 + \frac{J + J_{Ph}}{J_{01,i}}\right]$$

which represents the voltage of the top sub cell (i) as a function of the tandem cell's output current  $J$ . To find an equation for the bottom sub cell's (j) voltage, we can add the expression for the LC current (Eq. 23) to the right side of Eq. 21, and then take the inverse again to find

$$V_j(J) = \frac{kT}{q} \ln\left[1 + \frac{J + J_{Ph} + J_{LC}}{J_{01,i}}\right] \quad \text{Eq. 24}$$

Plugging the equation for LC current (Eq. 23) into Eq. 24 gives the voltage of the bottom sub cell as

$$V_j(J) = \frac{kT}{q} \ln \left[ 1 + \frac{J + J_{Ph,2} + \eta_{i,j}(J + J_{Ph,1})}{J_{01,2}} \right] \text{ Eq. 25}$$

When we compare Eq. 25 and Eq. 23, we can see that adding the LC current into the bottom sub cell's photocurrent adds an extra " $\eta_{i,j}(J + J_{Ph,1})$ " term into the ln in Eq. 25. This extra term increases the bottom sub cell's voltage,  $V_j(J)$ . This suggests that stronger luminescent coupling (a larger  $\eta$ ) should increase the voltage of the bottom sub cell. This also predicts that LC increases the voltage of the entire tandem cell, since the tandem cell voltage is a sum of the individual cell junction voltages.

Equations 23 and 25 can be added together and then plotted to give the J vs V curves for the two junction tandem cell. The tandem cell's J(V) graph when the cell is top junction limited is shown below in Fig. 9, and the tandem's J(V) curve when the cell is bottom junction limited and current matched is plotted in Fig. 10. To understand the impacts of LC on the  $J_{sc}$ ,  $V_{oc}$ , and PCE, the LC efficiency  $\eta$  was varied between 0 and 0.9.

This image is under copyright. It can be viewed online in the publication "Analysis of Multijunction Solar Cell Current-Voltage Characteristics in the Presence of Luminescent Coupling" Friedman et al. Figure 2.

Fig. 9. (a) The J (current density in mA/cm<sup>2</sup>) vs voltage (in V) for the two junction tandem cell when it is top junction limited ( $J_1^{EXT} < J_2^{EXT}$ ). The maximum power point is shown as an x. The dotted line represents a cell with no LC between junctions, and the solid line is a tandem cell with a high ( $\eta = 0.9$ ) LC efficiency.

Fig. 10. (b) The JV curves of the two junction tandem cell when it is bottom junction limited (red curves) ( $J_1^{EXT} > J_2^{EXT}$ ) and the two junction tandem cell when it is current matched (green curves) ( $J_1^{EXT} = J_2^{EXT}$ ). Both cases have a curve with no LC ( $\eta = 0$ ) and strong LC ( $\eta = 0.9$ ).

From figures 9 and 10, the effects of LC on the tandem cell can be studied. The  $J_{sc}$  of a cell is the maximum current on the cell's JV curve, which happens at the point on the curve where  $V=0$ . For the top junction limited and current matched tandem cells, the  $J_{sc}$  of the tandem cell stay the same whether or not the cells experience LC. However, when the tandem cell was bottom junction limited, the tandem cell's  $J_{sc}$  increased by about 1 mA/cm<sup>2</sup> when the cell's LC efficiency  $\eta$  increased from 0 to 0.9. When the tandem cell is bottom junction limited, increasing LC increased the  $J_{sc}$  of the bottom sub cell, which increased the  $J_{sc}$  of the tandem cell as well.

Figures 9 and 10 can also show how the  $V_{oc}$  of the tandem cell changes when LC strength is varied. The  $V_{oc}$  of a junction is the maximum voltage on its JV curve. The top and bottom junction limited sub cells along with the current matched cell all had a slight increase in their  $V_{oc}$ s when the LC efficiency was increased. When LC efficiency increases, there are a

greater number of photons absorbed in the bottom junction, which should induce a higher potential across the bottom junction. Increasing the voltage across the bottom junction increases the voltage of the entire tandem cell, since the tandem cell's voltage is the sum of each of the individual sub cell voltages.

Finally, figures 9 and 10 can show the impacts of LC on the maximum power output of the two-junction tandem cell. The maximum power point of each of the six cell conditions is marked as an "X" on the curves in figures 9 and 10. For the tandem cell that was top junction limited, there was no difference in the maximum power point of the cell with and without LC. For the tandem cells that were bottom junction limited and current matched, the cells with strong LC had a slightly bigger (further to the right or higher up) maximum power point than the cell without LC. The maximum power point of the tandem cell increased most significantly with the increase in LC when the tandem cell was bottom junction limited. When the tandem cell is bottom junction limited, increasing LC increases the current output of the tandem cell, which increases the cell's power output.

Overall, figures 9 and 10 predict that introducing strong LC in two junction tandem solar cells can increase the  $J_{sc}$  and maximum power output of the cell when it is bottom junction limited.

To measure the impacts of luminescent coupling experimentally, the study "Analysis of Multijunction Solar Cell Current-Voltage Characteristics in the Presence of Luminescent Coupling" also synthesized GaInP-GaAs cells with varying top junction thicknesses and doping levels, and measured the cells'  $J_{sc}$ ,  $V_{oc}$ , and PCE. The method used to measure the effects of luminescent coupling on the GaInP-GaAs tandem cells is described in "Measuring IV Curves and Sub cell Photocurrents in the Presence of Luminescent Coupling". Sub cell photocurrents were measured using a xenon lamp with LEDs that emitted shorter (470 nm) and longer (850nm) wavelength light. The  $J_{sc}$  of both the GaInP-GaAs cells and a reference cell were then measured at each of these wavelengths. When the shorter wavelength of light from the lamp was incident on the cell, the researchers assumed that all of the light was absorbed by the top sub cell, and that the measured  $J_{sc}$  of the tandem cell was equal to the  $J_{sc}$  of the top sub cell. When the longer wavelength light from the lamp was incident on the cell, the researchers assumed that all of the light passed through the top sub cell and was absorbed by the bottom sub cell, and that the measured  $J_{sc}$  of the cell was the  $J_{sc}$  of the bottom sub cell. Once the  $J_{sc}$ s for each of the sub cells of both the GaInP-GaAs tandem cell and the reference cell were measured, the effects of luminescent coupling on the tandem cell's  $J_{sc}$  could be found by subtracting the reference cell's  $J_{sc}$  from the GaInP-GaAs tandem cell's  $J_{sc}$ . The difference was equal to the current boost created by the luminescent coupling. The resulting  $J_{sc}$ ,  $V_{oc}$ , and efficiency of the tandem are shown below in Fig. 11.

This image is under copyright. It can be viewed online in the publication "Analysis of Multijunction Solar Cell Current-Voltage Characteristics in the Presence of Luminescent Coupling" Friedman et al. Figure 5.

Fig. 11.  $V_{oc}$ ,  $J_{sc}$ , fill factor, and efficiency (PCE) of GaInP/GaAs tandem cells with weak luminescent coupling ( $\eta = 0$ ) and strong luminescent coupling ( $\eta = 0.9$ ) as functions of the top junction thickness (GaInP layer).

For all thicknesses of the GaInP top junction, stronger luminescent coupling led to slightly (but not significantly) higher  $V_{oc}$ s for the tandem cell. The maximum  $V_{oc}$  of the cell occurs at a thickness of  $0.5 \mu\text{m}$ , but increasing the top junction thickness to  $1.5 \mu\text{m}$  only negligibly decreases the  $V_{oc}$ .

LC had varying impacts on the cells'  $J_{sc}$ s. When the top junction thickness was between  $0.5\text{-}1\mu\text{m}$ , the tandem cell was top junction limited and LC did not impact the cell's  $J$  or  $J_{sc}$ . Once the top sub cell thickness is greater than  $1.0 \mu\text{m}$ , the cell becomes bottom junction limited, since less of the light incident on the cell passes through the top junction and becomes incident on the bottom junction of the cell. Once the cell is bottom junction limited (when the top cell thickness increases), increasing luminescent coupling keeps the total  $J$  and  $J_{sc}$  of the bottom sub cell from decreasing, and the tandem cell  $J$  and  $J_{sc}$  is greater for higher luminescent coupling strengths.

When luminescent coupling was weak ( $\eta = 0$ ), the  $J_{sc}$  of the tandem solar cell is equal to the smallest  $J_{sc}$  coming from one of the sub cells. In this case, once the top junction reaches a high enough thickness and the cell becomes bottom junction limited (the bottom sub cell's  $J_{sc}$  is smaller than the top sub cell's  $J_{sc}$ ), the  $J_{sc}$  of the tandem cell is equal to the bottom sub cell's  $J_{sc}$ . However, when the tandem cell is bottom junction limited and luminescent coupling is increased ( $\eta > 0$ ), the current from luminescent coupling boosts the  $J_{sc}$  of the bottom sub cell, and the  $J_{sc}$  of the tandem cell increases. This is shown in Fig. 12 below. Stronger luminescent coupling mitigates the decrease in the tandem cell's  $J_{sc}$  when the cell is bottom junction limited, allowing the top sub cell to stay thicker without decreasing the tandem cell's  $J_{sc}$ . "Thus, luminescent coupling mitigates and can in principle eliminate the need for optical thinning in multijunction solar cells" [3].

This image is under copyright. It can be viewed online in the publication "Analysis of Multijunction Solar Cell Current-Voltage Characteristics in the Presence of Luminescent Coupling" Friedman et al. Figure 4.

Fig. 12. The current density output by the top junction ( $J_1^{\text{EXT}}$ ) and bottom junction ( $J_2^{\text{EXT}}$ ), and the current density output by the bottom junction when the cell has a LC efficiency of 0.9 ( $J_2^{\text{Tot}}$ ).

By measuring the  $J_{sc}$  and  $V_{oc}$  of GaInP-GaAs tandem cells with strong and weak luminescent coupling, the paper found that for top junction limited cells, strong luminescent coupling increased the  $V_{oc}$  of the cell. For bottom junction limited cells, strong luminescent

coupling increased the  $V_{oc}$  and PCE of the cell. Stronger LC could eliminate the need to have a thin top sub cell layer to keep the J and PCE of the tandem cell higher, which is an advantage of LC. Understanding the impacts of LC guides the optimal thickness of the top cell layer for tandem cells. This finding can likely be generally applied to monolithic tandem solar cells in general, since regardless of the materials used, it seems as if increasing the thickness of the top layer can increase the amount of light absorbed in the top layer, decreasing the amount of light incident on the bottom layer(s) and causing the tandem cell to be bottom junction limited. If the tandem cell has strong luminescent coupling efficiency between the top and bottom layers, excess current generated in the top junction can be transferred to the bottom junction, which increases the current output and efficiency of the tandem cell. This could suggest that in perovskite tandem solar cells, perovskite top layers could be slightly thicker while still maintaining high cell currents and efficiencies.

### **Effects of Luminescent Coupling in Perovskite Tandem Solar Cells**

The effects of luminescent coupling were also studied in silicon-perovskite tandem solar cells in the study “Perovskite/Silicon Tandem Solar Cells: Effect of Luminescent Coupling and Bifaciality”. In the study, researchers simulated luminescent coupling between the perovskite and silicon layers. The results predict that luminescent coupling will increase the PCE and power output of the tandem cells when the perovskite layer bandgap is smaller.

In silicon-perovskite tandem solar cells, perovskite is used as a top layer since it has a higher bandgap than silicon, allowing it to absorb higher energy photons. Lower energy photons pass through the perovskite top-layer and can be absorbed by a smaller-band gap silicon layer. The effects of luminescent coupling on silicon-perovskite tandem cells are studied using optical simulations in GenPro4 by Jäger et. al. in “Perovskite/Silicon Tandem Solar Cells: Effect of Luminescent Coupling and Bifaciality”. The simulations measured the power output of the cell when the bandgap of the perovskite top cell layer and luminescent coupling were varied. The results are shown in the figure below.

This image is under copyright. It can be viewed online in the publication “Perovskite/Silicon Tandem Solar Cells: Effect of Luminescent Coupling and Bifaciality” Jager et al. Figure 3.

Fig. 5. Graph of the output power density of the tandem cell (in  $\text{mW}/\text{cm}^2$ ) vs the top cell band gap (in eV), when the luminescent coupling efficiency was varied from 0-100%.

When luminescent coupling was increased, the power conversion output of cells with lower perovskite band gaps increased. When the perovskite band gap is low, photons with lower energy can be absorbed in that layer, and less light passes through the top layer. This reduces the amount of light incident on the bottom layer, reducing the bottom layer’s current and the tandem cell becomes bottom junction limited (the current output by the entire cell is equal to the current coming from the bottom layer). Increasing LC did not change the optimal bandgap of the perovskite layer, but it greatly increased the power output of the cell when the perovskite layer had a low bandgap. For all strengths of luminescent coupling, the optimal bandgap of the perovskite layer was 1.71 eV.

## **Conclusion**

The use of perovskites and strong luminescent coupling in tandem solar cells can create higher efficiency solar cells. Since perovskites are ferroelectric, they are able to hold a voltage without the application of an external electric field, which assists charge separation and can boost the voltage across a solar cell. Perovskites are also of interest for use in tandem solar cells because they can have narrow and tunable bandgaps. Tandem solar cells contain multiple absorber layers that each absorb a different range of the solar spectrum, allowing them to absorb more light and potentially have a higher power output than single junction cells.

One important effect in perovskite tandem solar cells (and tandem solar cells in general) is luminescent coupling, which happens when luminescent photons emitted in the top junction of a cell are absorbed in lower tandem cell layers. Luminescent coupling impacts the  $J_{sc}$ ,  $V_{oc}$ , optimal thickness, and the efficiency of tandem solar cells, so measuring luminescent coupling and understanding luminescent coupling in the cells can guide the cells' design. The effects of luminescent coupling can be measured using simulations in GenPro4, analytically by using the two-diode model, and experimentally by measuring the  $J_{sc}$ ,  $V_{oc}$ , and efficiency of two junction tandem cells. Luminescent coupling allows monolithic tandem cells to output a higher current and power when they are bottom junction limited, have thicker top cell layers, or have top layers with low bandgaps. Overall, tandem solar cells that have strong luminescent coupling and are made of perovskite materials can potentially output more power than other tandem solar cells.

## Sources

- 1: Li, Huilin, et al. “Photoferroelectric Perovskite Solar Cells: Principles, Advances and Insights.” *Nano Today*, Elsevier, 13 Jan. 2021, [www.sciencedirect.com/science/article/pii/S1748013220302322#:~:text=Ferroelectricity%20of%20a%20perovskite%20material,have%20non%2Dcentrosymmetric%20unit%20cell.](http://www.sciencedirect.com/science/article/pii/S1748013220302322#:~:text=Ferroelectricity%20of%20a%20perovskite%20material,have%20non%2Dcentrosymmetric%20unit%20cell.)
- 2: Singh, Ranbir, and Mritunjaya Parashar. “Origin of Hysteresis in Perovskite Solar Cells.” *AIP Publishing*, 30 Dec. 2020, [pubs.aip.org/books/monograph/70/chapter/20664776/Origin-of-Hysteresis-in-Perovskite-Solar-Cells](https://pubs.aip.org/books/monograph/70/chapter/20664776/Origin-of-Hysteresis-in-Perovskite-Solar-Cells).
- 3: Friedman, Daniel, Geisz, John, Steiner, Myles. “Analysis of Multijunction Solar Cell Current – Voltage Characteristics in the Presence of Luminescent Coupling”
- 4: Jager, Klaus, et al. “Perovskite/Silicon Tandem Solar Cells: Effect of Luminescent Coupling and Bifaciality”, 12 Dec. 2020, <https://onlinelibrary.wiley.com/doi/10.1002/solr.202000628>
- 5: Liu, Zhe. “Optical loss analysis of silicon wafer based solar cells and modules”, Dec. 2016, [https://www.researchgate.net/publication/319141094\\_Optical\\_loss\\_analysis\\_of\\_silicon\\_wafer\\_based\\_solar\\_cells\\_and\\_modules](https://www.researchgate.net/publication/319141094_Optical_loss_analysis_of_silicon_wafer_based_solar_cells_and_modules)
- 6: Kittel, Charles. *Introduction to Solid State Physics*. John Wiley and Sons.
- 7: Tayagaki, Takeshi et. al. “Impact of nanometer air gaps on photon recycling in mechanically stacked multi-junction solar cells”, Jan. 2019, [https://www.researchgate.net/publication/330301719\\_Impact\\_of\\_nanometer\\_air\\_gaps\\_on\\_photon\\_recycling\\_in\\_mechanically\\_stacked\\_multi-junction\\_solar\\_cells](https://www.researchgate.net/publication/330301719_Impact_of_nanometer_air_gaps_on_photon_recycling_in_mechanically_stacked_multi-junction_solar_cells)
- 8: David L. Chandler | MIT News Office. “Explained: Why Perovskites Could Take Solar Cells to New Heights.” *MIT News | Massachusetts Institute of Technology*, [news.mit.edu/2022/perovskites-solar-cells-explained-0715](https://news.mit.edu/2022/perovskites-solar-cells-explained-0715). Accessed 25 Apr. 2024.
- 9: Griffiths, David. *Introduction to Electrodynamics*. Pearson, 2013.
- 10: “Electric Polarization.” *Encyclopedia Britannica*, Encyclopædia Britannica, inc., [www.britannica.com/science/electric-polarization](http://www.britannica.com/science/electric-polarization). Accessed 25 Apr. 2024.

- 11: Liu, Zhezhi et al. "A review of modeling of luminescent coupling effect in multi-junction solar cell based on diode equation", <https://academic.oup.com/ijlct/article/16/4/1519/6364881>
- 12: *PVEducation*, [www.pveducation.org/](http://www.pveducation.org/). Accessed 25 Apr. 2024.
- 13: Bellini, Emiliano. "Kaust Claims 33.7% Efficiency for Perovskite/Silicon Tandem Solar Cell." *Pv Magazine International*, 30 May 2023, [www.pv-magazine.com/2023/05/30/kaust-claims-33-7-efficiency-for-perovskite-silicon-tandem-solar-cell/](http://www.pv-magazine.com/2023/05/30/kaust-claims-33-7-efficiency-for-perovskite-silicon-tandem-solar-cell/).
- 14: "Solar Photovoltaic Cell Basics." *Energy.Gov*, [www.energy.gov/eere/solar/solar-photovoltaic-cell-basics](http://www.energy.gov/eere/solar/solar-photovoltaic-cell-basics). Accessed 25 Apr. 2024.
- 15: Kitanaka, Yuuki, et al. "Polarization Twist in Perovskite Ferrielectrics." *Nature News*, Nature Publishing Group, 2 Sept. 2016, [www.nature.com/articles/srep32216](http://www.nature.com/articles/srep32216).
- 16: "6.1.1: Dielectric Polarization." *Engineering LibreTexts*, Libretexts, 4 Nov. 2022, [eng.libretexts.org/Workbench/Materials\\_Science\\_for\\_Electrical\\_Engineering/06%3A\\_Thermal\\_Optical/6.01%3A\\_Optical\\_Properties/6.1.01%3A\\_Dielectric\\_Polarization](http://eng.libretexts.org/Workbench/Materials_Science_for_Electrical_Engineering/06%3A_Thermal_Optical/6.01%3A_Optical_Properties/6.1.01%3A_Dielectric_Polarization).
- 17: Park, Nam-Gyu. "Perovskite solar cells: An emerging photovoltaic technology", [https://www.researchgate.net/publication/264900172\\_Perovskite\\_solar\\_cells\\_An\\_emerging\\_photovoltaic\\_technology](https://www.researchgate.net/publication/264900172_Perovskite_solar_cells_An_emerging_photovoltaic_technology)